Assessment of Aircraft Icing Potential and Maximum Icing Altitude from Geostationary Meteorological Satellite Data

GARY P. ELLROD*

NOAA/NESDIS/Center for Satellite Applications and Research, Camp Springs, Maryland

ANDREW A. BAILEY

Raytheon Information Solutions, Camp Springs, Maryland

(Manuscript received 16 September 2005, in final form 28 June 2006)

ABSTRACT

A satellite product that displays regions of aircraft icing potential, along with corresponding cloud-top heights, has been developed using data from the Geostationary Operational Environmental Satellite (GOES) imager and sounder. The icing product, referred to as the Icing Enhanced Cloud-top Altitude Product (ICECAP), is created hourly for the continental United States and southern Canada, and is color coded to show cloud-top altitudes in 1.9-km (6000 ft) intervals. Experimental ICECAP images became routinely available on the Internet during the spring of 2004. Verification of separate ICECAP components (imager icing potential and sounder cloud-top heights) using aircraft pilot reports (PIREPs) indicates that the product provides useful guidance on the spatial coverage and maximum altitude of current icing conditions, but not icing intensity, stratification, or minimum altitude. The imager icing potential component of ICECAP was compared with the operational 40-km resolution National Weather Service (NWS) current icing potential and NWS Airman's Meteorological Advisories via the NOAA Real-Time Verification System, while GOES cloud-top heights were compared with altitudes of moderate or greater icing from PIREPs. Benefits and deficiencies of the GOES icing product are discussed.

1. Introduction

Geostationary and polar-orbiting meteorological satellites have been used to help detect supercooled clouds that cause in-flight icing since the early 1990s (Curry and Liu 1992; Ellrod 1996; Vivekanandan et al. 1996; Thompson et al. 1997; Smith et al. 2000). Satellite data have a number of distinct benefits in the analysis of aircraft icing such as multispectral capabilities, frequent sampling (geostationary satellites only), and excellent spatial coverage and resolution. The five-channel Geostationary Operational Environmental Satellite (GOES) imager (Menzel and Purdom 1994; Ellrod et al. 1998) provides five spectral bands (see Table 1) with moderate resolution (1–8 km) that are useful for measuring or inferring conditions conducive to icing on a frequent basis (15–30 min). The GOES sounder (Menzel et al. 1998) is an independent instrument that has many more infrared (IR) bands (18), but with lower horizontal resolution (10 km) and less frequent sampling (1 h at best) (Table 2). The Advanced Very High Resolution Radiometer (AVHRR) on the National Oceanic and Atmospheric Administration (NOAA) polar-orbiting satellites has a suite of spectral channels similar to the GOES imager. Although the two operational NOAA satellites provide only four observations per day at midlatitudes, AVHRR has better subpoint resolution in the IR bands than GOES (1 km versus 4 km at nadir). Due to its more frequent sampling, however, GOES is the preferred instrument for observing changes in mesoscale conditions leading to aircraft icing, and is the source of data for the products described in this paper.

While icing cannot be observed explicitly from satellite data, parameters such as cloud-top temperature and visible cloud reflectance (albedo) can be used to infer icing potential. Longwave infrared (LWIR) channels (10–13 μm) are used to obtain cloud-top temperature, and also to help distinguish thin ice clouds from dense

* Retired.

Corresponding author address: Gary Ellrod, P.O. Box 240, Granby, CT 06035.
E-mail: gary.ellrod@gmail.com

DOI: 10.1175/WAF984.1

© 2007 American Meteorological Society

TABLE 1. GOES imager spectral bands (changes in boldface type).

Band	*GOES-8–11* Wavelength (μm)	*GOES-8–11* Resolution (km)	*GOES-12–15* Wavelength (μm)	*GOES-12–15* Resolution (km)
1	0.6	1	0.6	1
2	3.9	4	3.9	4
3	6.7	8	**6.5**	**4**
4	10.7	4	10.7	4
5	12.0	4	—	—
6	—	—	**13.3**	**8**

TABLE 2. GOES sounder channel characteristics.

Channel	Detector type	Spectral peak (μm)	Purpose
1	Longwave	14.71	Stratosphere temperature
2		14.37	Tropopause temperature
3		14.06	Upper-level temperature
4		13.64	Midlevel temperature
5		13.37	Low-level temperature
6	Window	12.66	Total PW
7		12.02	Surface temp of water
8		11.03	Surface temp
9	Ozone	9.71	Total ozone
10	Water vapor	7.43	Low-level moisture
11		7.02	Midlevel moisture
12		6.51	Upper level moisture
13	Shortwave	4.57	Low-level temperature
14		4.52	Mid-level temperature
15		4.45	Upper level temperature
16	Nitrogen	4.13	Boundary layer temperature
17	Shortwave window	3.98	Surface temperature
18		3.74	Surface temperature, H_2O
19	Visible	0.70	Clouds

liquid water clouds to reduce false detection. Geostationary satellite data can thus observe changes in the horizontal extent of supercooled clouds, and can be used to help reduce the overprediction of icing commonly found when using numerical model data (Thompson et al. 1997).

The principal weakness of IR remote sensing techniques is the inability to observe supercooled clouds that are obscured by higher cirrus cloud layers. Also, since satellite IR techniques only observe cloud tops, icing conditions embedded within deep cloud systems cannot be observed directly. It has been shown, however, that liquid water droplets tend to accumulate near the tops of stratiform cloud layers (Rauber and Tokay 1991), thus allowing GOES techniques to be effective in many situations. Another shortcoming of satellite remote sensing is that icing below thermal inversions in which cloud-top temperatures are >0°C cannot be detected, such as in conditions where freezing rain or drizzle occurs.

Shortwave IR (SWIR) channels (near 4.0-μm wavelength) also help in assessing cloud phase by means of differences in emitted IR radiance between ice and water clouds at night, and solar reflectance differences during daytime. Water clouds have distinct brightness temperature differences (BTDs) in the LWIR–SWIR bands from those of ice clouds at night (e.g., Ellrod 1995) and can easily be discriminated using appropriate thresholds. Clouds containing water droplets are usually at least 1 K cooler in the SWIR than the LWIR channels at night, while the opposite is true of ice clouds. During daylight hours, SWIR data contain contributions from both emitted thermal and reflective solar energy. Solar reflectance overwhelms the radiative thermal component throughout much of the daytime period, resulting in more difficulty in using SWIR data than the LWIR channels. However, since water droplets are more reflective than ice cloud particles or snow- and ice-covered surface terrain at 4.0 μm, discrimination of cloud phase is possible using BTD techniques (Allen et al. 1990) or shortwave reflectance (Lee et al. 1997). Daytime SWIR − LWIR BTD values are usually very large for water clouds, typically reaching 30–40 K near midday. While SWIR − LWIR BTD values for ice clouds are also positive, discrimination from liquid phase clouds is still possible as long as the ice clouds are thin.

Experimental GOES icing products that are available from the National Environmental Satellite, Data, and Information Service (NESDIS) are able to provide useful information on the horizontal coverage of supercooled clouds (Ellrod 1996), but to date there has been no satellite-based information on the altitude of icing. This paper describes improved techniques that have been developed to help determine icing potential from the GOES imager, integrated with cloud-top heights from the GOES sounder.

2. GOES icing and cloud-top products

The NESDIS composite icing and cloud-top product is referred to as the Icing Enhanced Cloud-top Altitude Product (ICECAP). The product consists of icing potential determined from the 5-channel GOES imager, combined with cloud-top heights extracted from the 19-channel GOES sounder (Menzel et al. 1998). Table 1 shows imager spectral bands for *GOES-8–11*, as well as the channels available for *GOES-12* (the current operational eastern spacecraft) through *GOES-15*. One major change in the newer imagers (beginning with *GOES-12*) is the substitution of a CO_2 absorption chan-

nel centered near 13.3 μm (with 8-km resolution) for the longwave 12-μm window. This change affects the way the icing algorithm must discriminate thin cirrus for the reduction of false detection. The procedures used for determining each component of the product will be discussed separately in the following sections.

a. Icing potential estimated from the GOES imager

Conditions favorable for airframe icing, along with the effects of icing on aircraft performance have been studied extensively (e.g., World Meteorological Organization 1954; Sand et al. 1984; Hansman 1989; Politovich 1996). The most important ingredients for significant (moderate to severe) in-flight icing can be summarized as 1) liquid-phase clouds, 2) temperatures in the 0° to −20°C range, 3) large droplet mean volume diameters (MVDs) (>30 μm), 4) weak upward motion to replenish the available supercooled water, 5) large liquid water content (LWC) (>0.2 g m^{-3}), and 6) thick, extensive cloud systems resulting in longer in-flight exposure to icing conditions. Temperatures at the warmer end of the preferred icing range (0° to −10°C) are typically associated with the more hazardous moderate to severe clear or mixed icing events with large MVD and high LWC values (Politovich 1996). At colder temperatures (<−15°C), stratiform clouds tend to have larger concentrations of ice particles, lower LWC, small MVD, and therefore, lower icing risk. Due to the complex meteorological and cloud physical conditions often found in icing situations, diagnosis and forecasting of in-flight icing are a tremendous challenge. A discussion of the procedures used by aviation forecasters in the United States is given in Schultz and Politovich (1992).

The optimum conditions just described largely explain the high icing vulnerability of aircraft operating at lower altitudes such as general aviation (GA) and commuter class aircraft: a study of aircraft icing accidents for a 19-yr period (1982–2000) by Petty and Floyd (2004) showed that GA aircraft accounted for 80.6% of all airframe icing accidents, while commuter class aircraft accounted for 17.6% of icing accidents. Thus, less than 2% of icing accidents involved large commercial jet aircraft.

Since 1996, experimental products that show the potential for aircraft icing have been derived from GOES data (Ellrod 1996; Vivekanandan et al. 1996; Smith et al. 2000). An explicit parameter related to icing potential that can be measured from GOES is the IR cloud-top temperature (CTT), obtained from the 10.7-μm "window" channel 4 (CH4) (Table 1). The absolute accuracy of CTT from the GOES imager is stated as ≤1 K (Space Systems Loral 1996). The cloud-top temperature range used in the NESDIS product to denote possible icing conditions is −1° to −30°C, which is a slightly broader range than that typically associated with optimum icing conditions. The colder temperature threshold captures a greater percentage of icing cases, as it accounts for the cooling with height that is typically found in deeper cloud layers.

Since the use of cloud-top temperature alone may result in false icing signatures, additional techniques must be used to filter out satellite pixels not representative of supercooled clouds. For example, thin cirrus may have an IR temperature in the optimum range, but is obviously not capable of creating an icing hazard for aircraft. Likewise, cold snow-covered ground under clear-sky conditions must be identified and eliminated as a possible icing cloud.

1) DAYTIME ICING DETECTION

As previously mentioned, during daytime, the shortwave IR channel (CH2 on GOES) contains contributions from both thermal emission and solar reflectance. Visible channel (CH1) reflectance depends on the cloud thickness (optical depth) and liquid water content while shortwave IR reflectance responds primarily to cloud droplet size and solar zenith angle (e.g., Allen et al. 1990). Since the drop size sensitivity in shortwave IR data is most pronounced at diameters <30 μm (Kleespies 1995), useful information on cloud droplet size and icing intensity from GOES data is limited, and not currently accounted for in the NESDIS product.

During the daytime, visible data are corrected for satellite viewing angle using a program developed at the National Weather Service (NWS) Aviation Weather Center (AWC). This correction normalizes the visible data so that results are consistent over a larger area. The test for liquid water clouds is then performed using empirical thresholds based on CH2 − CH4 BTD and corrected CH1 brightness values. The thresholds were obtained from discriminant analysis of 114 *GOES-12* observations in four spectral bands for various cloud and surface types (Fig. 1), for which band-4 IR temperatures were between −1° and −30°C. The data were collected on 26 days between July 2003 and February 2004. All data were obtained during daylight hours in varying amounts of solar illumination, a few within 2 h after sunrise or before sunset. Liquid-phase clouds, confirmed by aircraft pilot reports of moderate or greater icing (denoted by open circles), were assumed to be present in 62 of these cases. Based on these data, icing conditions were associated with a corrected visible brightness count value of 155 or more (albedo ≥ 37%), while the CH2 − CH4 BTD also exceeded 10 K (Fig. 1). All other data points represent the absence of icing conditions. The large brightness values

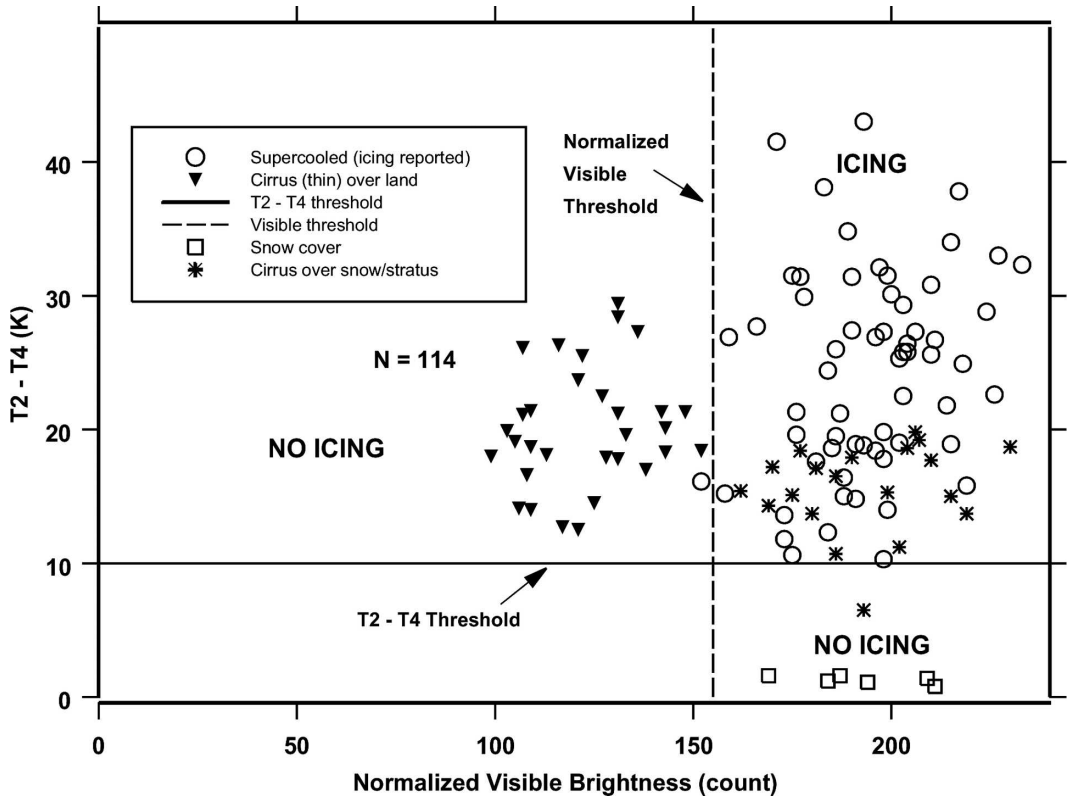

FIG. 1. Scatterplot showing CH2 − CH4 BTD (K) vs normalized visible channel brightness count for various cloud and surface types with $0° < T_4 < -30°C$. Presence of supercooled clouds was verified by aircraft icing reports. Horizontal and vertical lines are used as empirical thresholds for identifying clouds with icing potential.

for supercooled clouds makes physical sense, since water droplets scatter incoming sunlight more effectively than ice clouds or bare land. The CH2 − CH4 BTD values are likewise due to stronger reflectance by water clouds in the shortwave band (Allen et al. 1990).

Situations where cirrus clouds may be difficult to eliminate as potential supercooled water clouds were discussed by Schmidt et al. (1995) based on their simulations of GOES and AVHRR SWIR − LWIR BTD for ice clouds composed of hexagonal crystals. Large daytime simulated BTD values were observed for ice clouds whose particle sizes were small (4 μm), optical depths large (>1.0), and especially when the clouds overlaid reflective surfaces such as quartz sand. Many of these situations are eliminated using either the CTT or minimum albedo tests previously described. The threshold tests shown in Fig. 1 work well except for situations where there are thin cirrus clouds overlying either warm stratocumulus clouds or a snow cover (denoted by asterisks) and the CH4 CTTs meet the icing criteria. In those cases, it is not possible to completely eliminate false icing signatures without use of multispectral IR methods, since visible albedo values are similar to those for nonobscured water clouds. Our approach to these problems using the *GOES-12* channels is described in section 2a(3) below.

2) NIGHTTIME ICING DETECTION

At night, cloud phase is determined by a CH4 − CH2 BTD threshold similar to the one used in the nighttime IR product that identifies lower-level water clouds, including fog (e.g., Eyre et al. 1984; Ellrod 1995). At night, the typical CH4 − CH2 BTD threshold for the presence of a low cloud is ≥2.5 K. The optimum cloud–no-cloud threshold is slightly smaller (1–2 K) for clouds containing larger water droplets, such as maritime stratocumulus (Lee et al. 1997). However, a lower CH4 − CH2 BTD threshold introduces more CH2 instrument noise when subfreezing surface temperatures occur, resulting in speckled images and interpretation difficulties over land during winter months. There can also be false detection from low-emissivity desert soils such as those found in the southwestern United States (Saunders and D'Aria 1994). For this reason, the 2.5-K BTD threshold is used for the GOES icing product. The sensitivity of the shortwave IR channel to thin cirrus ob-

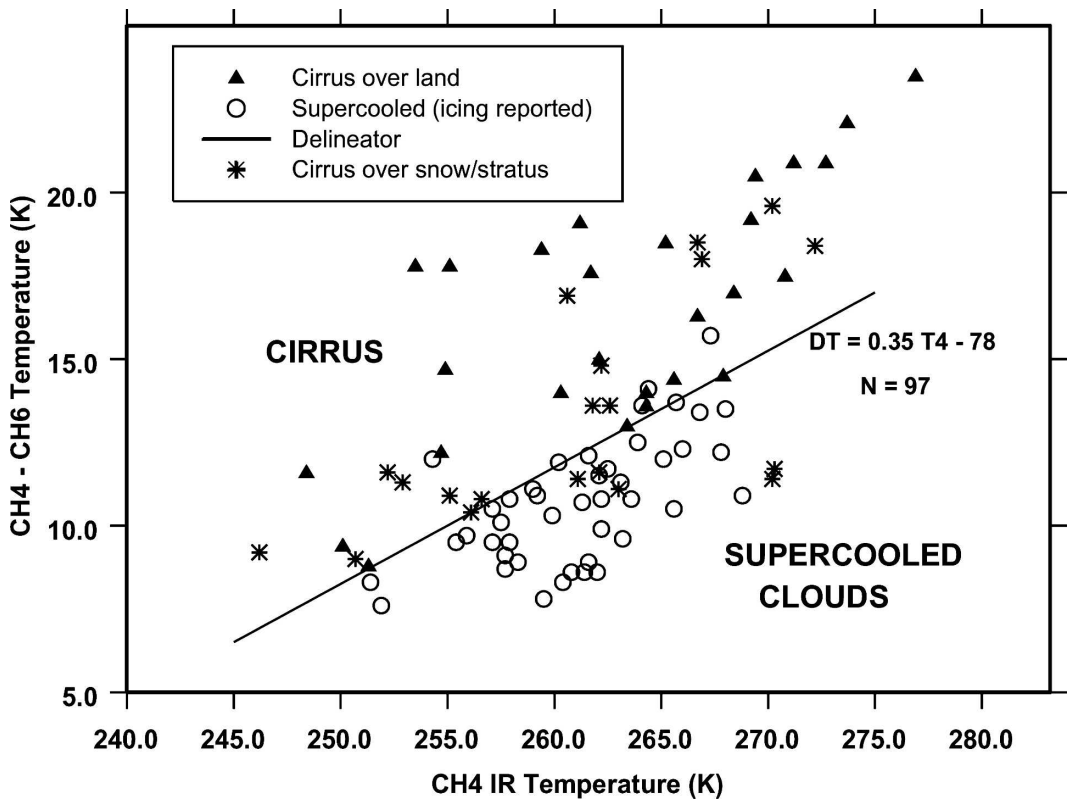

FIG. 2. CH4 − CH6 IR brightness temperature difference (K) from *GOES-12* for the indicated cloud types plotted vs CH4 temperature (K). Empirically determined line helps to discriminate false icing produced by thin cirrus (triangles and stars) from supercooled clouds (circles).

scures lower stratiform clouds and results in less effective detection of icing conditions at night overall.

3) CIRRUS DISCRIMINATION DAY AND NIGHT

To minimize false icing reports caused by cirrus during both day and night, a "split window" approach was used with *GOES-8–10* (Ellrod 1996). The CH4 − CH5 (12.0 μm) BTD was found to be ≥1 K for cirrus clouds, and <1 K for other cloud types or clear conditions, similar to previous findings (e.g., Inoue 1987). The *GOES-12* imager does not have the 12-μm channel, so the 13.3-μm channel (CH6) must be used instead. Since several future GOES spacecraft will have this same imager configuration, this is an important consideration until at least 2012, when GOES-R is expected to be launched. A slightly smaller subset (N = 97) of the dependent dataset shown in Fig. 1 was used to develop a new cirrus screening technique based on CH4 − CH6 BTD (Fig. 2). This new procedure was implemented during the late summer of 2004, but modified in January 2005 to correct for underdetection of icing pixels. An empirical line of discrimination shown in Fig. 2 is used to separate supercooled clouds from cirrus. The CH4 − CH6 BTD values equal to or larger than those determined by the following equation were likely associated with cirrus clouds and were eliminated from consideration:

$$\mathrm{BTD}_{46} = 0.35T_4 - 78. \quad (1)$$

This method is not as effective at large satellite zenith angles (>60°) due to greater thermal absorption at 13.3 μm than at 10.7 μm. However, a large portion of the false signatures due to thin cirrus over snow or warm low clouds can be eliminated in this manner.

4) GOES ICING ALGORITHM SUMMARY

A summary of the GOES icing product algorithm is shown by the flow diagram in Fig. 3. The approach used is similar to cloud clearing, where successive tests are applied to eliminate pixels that are likely to have clouds present. For this algorithm, we would like to remove conditions that are uncharacteristic of supercooled water clouds. The first step in the decision tree is to determine if the cloud-top temperature is in the appropriate range for icing (−1° to −30°C). The visible channel (CH1) brightness is then checked for an arbitrary mini-

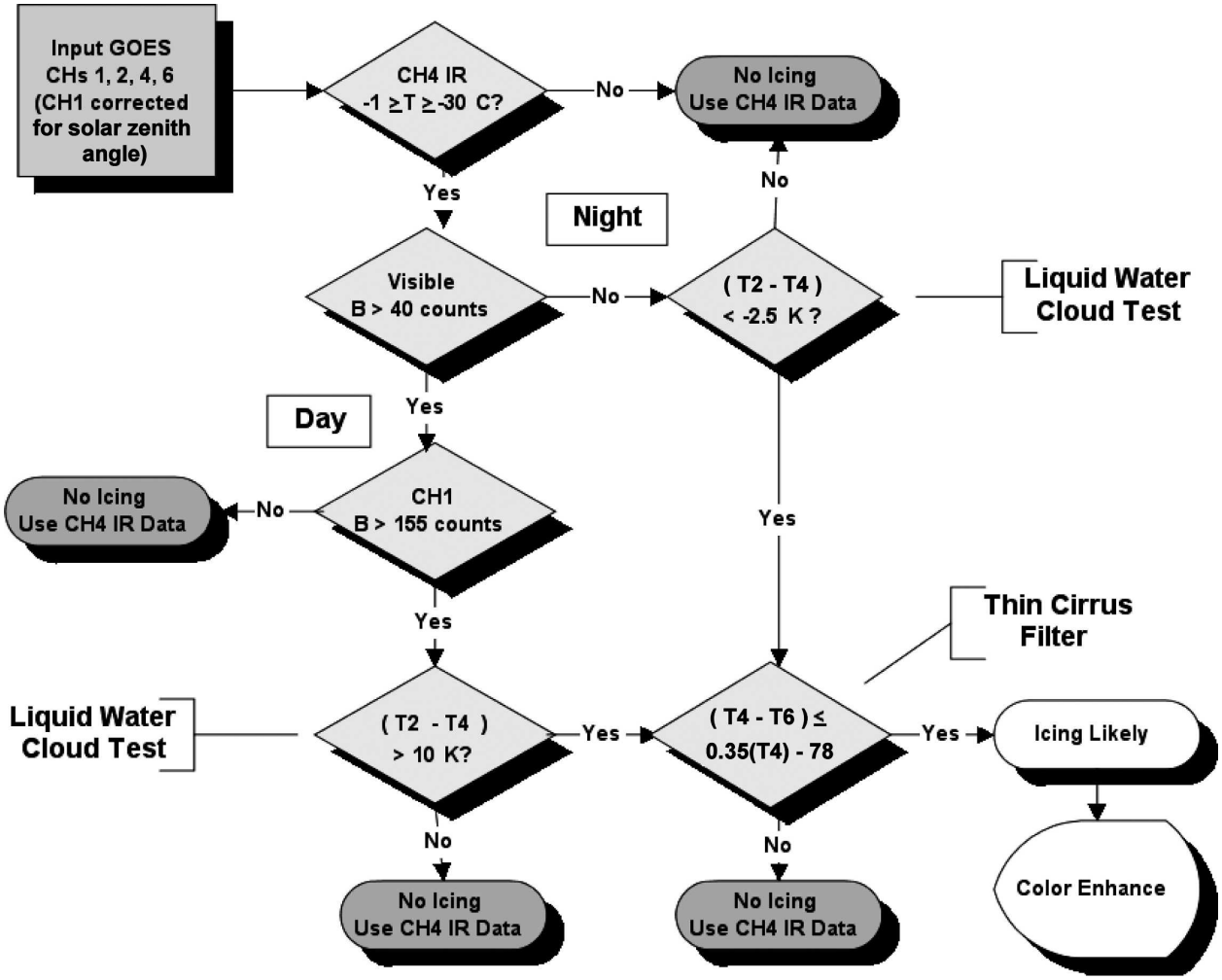

FIG. 3. Flow diagram showing algorithm used to generate the *GOES-12* imager icing product.

mum threshold value of 40 counts (albedo ~2.5%) to determine whether the day or night algorithm is applied. A minimum normalized CH1 brightness count threshold of 155 counts (albedo ~37%) is then applied (Fig. 1), combined with a minimum CH2 − CH4 BTD of 10 K to distinguish ice clouds (or bare ground) from water clouds during daytime. At night, a CH4 − CH2 BTD threshold of 2.5 K is used to identify liquid water clouds since it is the only information available to determine cloud phase. A screening technique based on CH4 − CH6 (Fig. 2) (or CH4 − CH5 for *GOES-10*) is then used to determine the likelihood of thin cirrus. If cirrus is present, that pixel is eliminated from further consideration of potential icing conditions. For pixels where all tests for icing fail, the CH4 IR data are substituted into the product at that location. The final product is color enhanced to show areas where all of the icing threshold tests were positive, with specific colors showing the cloud-height categories determined from the sounder's Cloud-top Product (CTP).

b. Cloud-top heights obtained from the GOES sounder

The other component of ICECAP is cloud-top height determined from the GOES Cloud-top Product (CTP), which has been generated from the sounder since the mid-1990s (Menzel et al. 1998). The CTP algorithm uses internal tests for the presence of 1) clear pixels based on comparisons with surface temperature data, 2) opaque clouds, and 3) semitransparent clouds.

If opaque clouds are determined to be present, an IR window technique is used to determine cloud-top height by matching the IR cloud-top temperature (CTT) to a numerical prediction model first-guess temperature profile. For low stratus clouds, the associated cloud-top height is determined by finding the first CTT

match to the first guess by searching from the ground up, whereas middle- and high-cloud matches are made by means of temperature comparisons from the top down. This approach has resulted in a significant improvement in estimates of low cloud-top heights (Schreiner et al. 2002).

If the clouds are semitransparent and located in the middle and upper troposphere (<700 hPa), the cloud-top height is estimated using the CO_2 slicing technique (CST) (Menzel et al. 1983). The CST is a physical relationship based on a special version of the radiative transfer equation that employs radiances from the sounder IR window band at 11 μm and CO_2 absorption bands from 13 to 15 μm. The main assumptions of the CST are 1) there is a single cloud layer present, 2) the cloud layer is opaque but infinitesimally thin (thus allowing application to semitransparent clouds), and 3) the emissivity of the cloud is the same in both spectral ranges. Since supercooled clouds that produce aircraft icing are opaque and of finite depth, and the CST describes mostly cirrus cloud layers, most CST-derived cloud-top heights are not used in the ICECAP product. One exception is when a thin cirrus layer overlies a stratiform cloud layer in the middle troposphere, usually resulting in an icing situation where the derived cloud-top height is too high (e.g., Wylie et al. 1994). Details on the GOES CTP generation and scientific approach are found in Schreiner and Schmit (2001) and Schreiner et al. (2002). The CTP has since become widely available to users via the World Wide Web (information available online at http://cimss.ssec.wisc.edu/goes/realtime/grtmain.html#ctop), and the NWS Advanced Weather Interactive Data Analysis System (AWIPS). Recent work on an imager CTP has shown considerable promise for possible use with ICECAP, as described in section 5b.

c. *ICECAP product generation*

The imager icing and sounder CTP programs are normally run separately due to differences in scan strategies, sensor resolutions, and data availability times. Processing to create the ICECAP has been combined into a single script that runs when the availability of all necessary satellite data is assured. The CTP is produced hourly via the GOES sounder processing system for both GOES-East (currently *GOES-12*) and -West (*GOES-11*), and the data are output in ASCII format to an Office of Research and Applications server at the World Weather Building, Camp Springs, Maryland. Processing for the continental U.S. (CONUS) scale ICECAP product is completed in less than 5 min. Since the northern extent of the CONUS sounder scan is limited to about 50°N, cloud-top height information for a large portion of southern Canada is missing, and is delineated as white in the images.

Currently, only imager data from *GOES-12* are used to determine icing risk in order to simplify the processing and provide a consistent data source, especially for the CH1 visible spectrum. The ICECAP program obtains the multispectral imager data for a subset of the Northern Hemisphere sector at three times, each an hour apart (thus spanning a 2-h period); normalizes the visible image data to correct for satellite viewing angle; performs the icing threshold tests (Fig. 3); composites all pixels that test positive for icing during the 2-h period; and finally blends the cloud-top data from the previous hour, to obtain the final product. If icing is likely, based on the imager icing algorithm, the program uses a nearest-neighbor approach to search for collocated sounder cloud-top height data.

The 2-h composite method allows for detection of icing for some locations that are occasionally obscured by broken higher cloud layers, and minimizes the effects of low-light conditions near the solar terminator that result in poor icing detection from either nighttime or daytime methods. Potential icing areas are assigned to an artificially low brightness count range (0–10), while the nonicing areas are assigned grayscale IR band-4 data as a background. Colors are assigned to icing pixels corresponding to cloud-top height intervals of 1.9 km (6000 ft), although the display of 0.9-km (3000 ft) intervals is possible. Pilot reports (PIREPs) are then overlain on the images, displaying the icing intensity code (1–6), aircraft type, and altitude (100s of ft). Experimental ICECAP images became available during the spring of 2004 on the NESDIS Operational Products Development Branch aircraft icing Web site (http://www.star.nesdis.noaa.gov/smcd/opdb/aviation/icg.html).

3. Example

Figure 4 shows an example of the CONUS-scale ICECAP product at 1315 UTC on 12 May 2005. Areas of potential icing and associated cloud-top heights are color coded according to the legend at the bottom of the image. Numerous reports of moderate or greater icing were observed along and to the north of a frontal system extending across the northern midwestern and northeastern United States. Much of the icing was associated with dense altostratus layers at altitudes between 3.3 and 6.4 km (10 000–20 000 ft). (i) Over New England, stratocumuli in cool northwesterly flow was producing some low-level icing conditions for general aviation aircraft. In the western United States, the nighttime algorithm was still in use, so some underde-

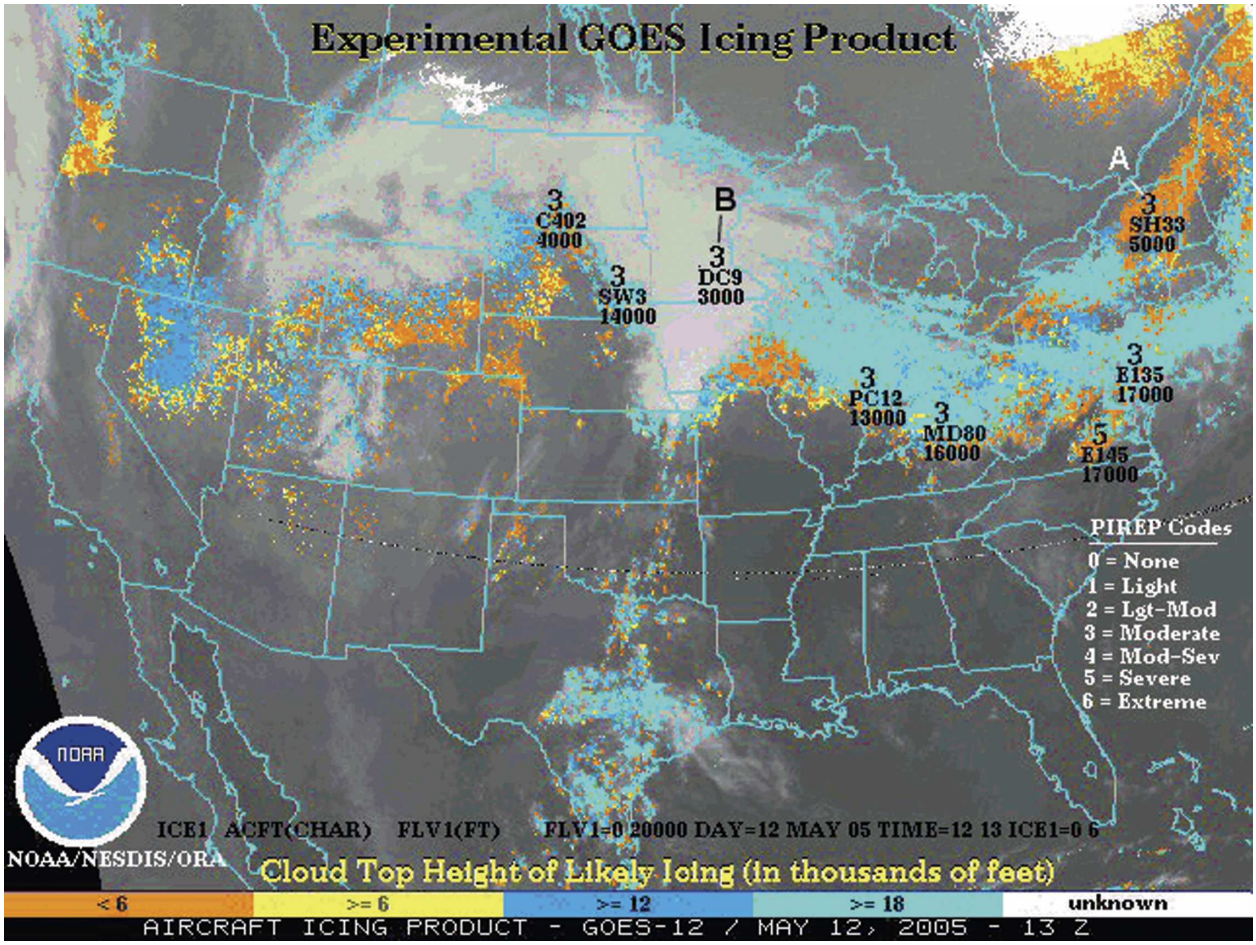

FIG. 4. A GOES ICECAP image for the CONUS is shown at 1315 UTC 12 May 2005. Legend shows cloud-top height color coded in intervals of 1.9 km (6000 ft). White areas indicate that icing is diagnosed but cloud-top heights are not available, such as in portions of southern Canada due to scan limitations of the GOES sounder. PIREP plots of icing intensity, aircraft type, and altitude (ft) are overlain.

tection was likely, based on inspection of later images (not shown). (ii) An example of the obscuration of icing conditions due to dense cirrus overcast is shown in the vicinity of Minneapolis, Minnesota. Overall, icing locations and altitudes as reported by aircraft were well depicted by the ICECAP.

Skew T–log$p$ profiles for Albany, New York (ALB), and Wilmington, Ohio (ILN), are shown in Fig. 5. The ALB profile reveals the pronounced subsidence and cold advection that limits the icing conditions to a shallow layer just below the inversion with a temperature range of 0° to −5°C. The ILN sounding indicates the presence of several cloud layers and a fairly deep subfreezing cloud layer above 600 hPa with temperatures between about −5° and −15°C.

4. Product verification

The two components of the product (imager icing and sounder CTP) have been verified separately using PIREP data. In addition to extensive validation of imager icing potential, the ICECAP cloud-top heights were validated to determine the ability to provide realistic upper bounds to icing layers in operational situations. Further descriptions of these comparisons follow in the sections below.

a. GOES imager icing potential

The GOES imager icing potential product was included in the NOAA/Earth System Research Laboratory's (ESRL's) Real-Time Verification System (RTVS) in early 2002. The RTVS uses the latest PIREPs, surface Meteorological Aerodrome Reports (METARs), and other types of observations to evaluate experimental products or operational algorithms that diagnose or forecast various aviation parameters (turbulence, icing, convection, etc.). These parameters may be derived from numerical model data, satellites, or other sensors (Mahoney et al. 2002). To perform the

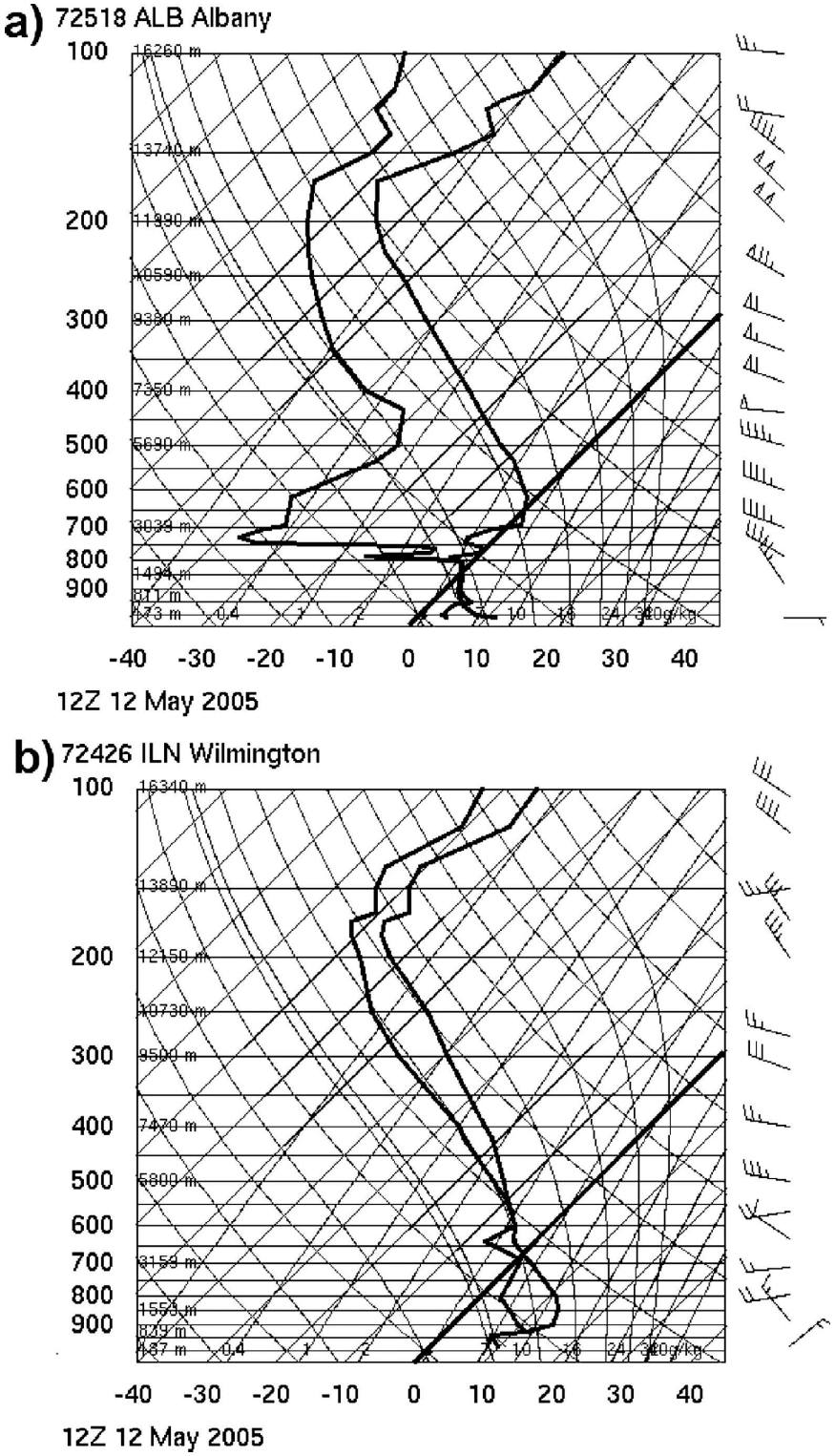

FIG. 5. Skew$T$–log$p$ diagrams showing radiosondes profiles of T (°C), T_d (°C), and wind direction and speed (kt) at 1200 UTC 12 May 2005 at (a) ALB and (b) ILN. The freezing isotherm (0°C) is shown by the thicker diagonal line. (Source—University of Wyoming Web site: http://weather.uwyo.edu/upperair/sounding.html.)

verification, the GOES imager icing product is remapped to correspond to the 40 km × 40 km resolution Rapid Update Cycle (RUC) model (Benjamin 1997), converted to netCDF format, and copied to ESRL via file transfer protocol (ftp). Thus, the area of the full resolution (4 km × 4 km) GOES imager icing product is reduced by a factor of 100 in order to conform to the RUC grid.

The GOES imager icing potential product was verified against the 40-km operational current icing potential (CIP) (McDonough and Bernstein 1999; Fowler et al. 2004; Bernstein et al. 2005). The CIP is based on output from the RUC model (temperature, relative humidity, etc.), along with surface METARs, PIREPs, radar reflectivities, and GOES IR data. RUC model temperature, relative humidity, vertical velocity, and explicit supercooled liquid water are used in the product. Satellite and radar data help to refine the volume of cloudiness as defined by the RUC. The cloud-top height estimate used in the RUC is determined from the CH4 IR data interpolated to the first-guess RUC model temperature–height profile. The CIP estimates the potential for in-cloud icing conditions based on a sliding scale from 0 to 1.

The sounder cloud-top height data included in ICECAP are not currently used by the RTVS. Therefore, a GOES pixel where icing is diagnosed is assigned to an altitude layer based on the PIREP altitude. A negative icing PIREP results in a missed diagnosis for the collocated GOES pixel in RTVS, regardless of altitude.

Statistics are generated by RTVS using parameters such as the probability of detection of icing occurrences (PODy), moderate or greater (MOGR) PODy, and POD for no icing (PODn). Some parameters, such as percent volume of airspace, cannot be provided for GOES icing due to missing information on icing bases and tops. Statistics can be viewed interactively for periods of time spanning individual days, months, or years in either graphical or tabular formats. Geographical areas are also user selectable for some types of data (the RTVS Web site address is http://rtvs.noaa.gov/index.html).

PODy is defined as

$$\mathrm{PODy} = \mathrm{YY}/(\mathrm{YY} + \mathrm{NY}), \tag{2}$$

where YY is the number of observed icing events that were detected by the product and NY is the number of icing events that were missed (not detected but observed). In this paper, PODy refers to moderate or greater intensity icing events identified by PIREPs. PODn gives the percentage of nonicing events correctly diagnosed and is defined as

$$\mathrm{PODn} = \mathrm{NN}/(\mathrm{NN} + \mathrm{YN}), \tag{3}$$

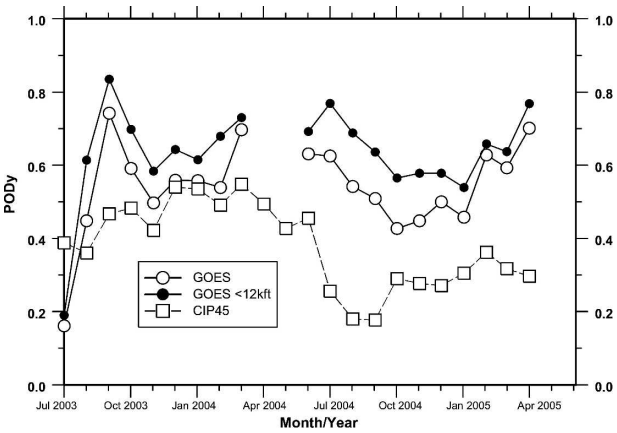

FIG. 6. PODy for the GOES imager icing product based on RTVS output for all levels (solid line, open circles), and for flight levels below 12 000 ft (3.8 km) (solid circles) compared with NWS 40-km CIP (dashed line) for the period from Jul 2003 through Apr 2005. CIP results were based on a threshold index value of 0.45.

where NN is the number of nonevents correctly determined by the product and YN is the number of nonevents where icing was diagnosed but not observed. The statistic (1 − PODn), combined with PODy, describes the ability of the product to discriminate between icing and nonicing situations by means of the true skill statistic (TSS) (Doswell et al. 1990) where

$$\mathrm{TSS} = \mathrm{PODy} + \mathrm{PODn} - 1. \tag{4}$$

The best possible combination of the two parameters (showing the highest skill) is PODy = 1, and 1 − PODn = 0. The curve resulting from a plot of PODy and 1 − PODn for a range of product thresholds describes the relative operating characteristics (ROC) of a forecast system (e.g., Mason and Graham 1999). Using this type of curve, a user could determine what PODy threshold would yield an acceptable false alarm rate (1 − PODn). While a nearly continuous ROC curve can be obtained from CIP data, only one point can be used to compare the GOES icing product, since it currently provides only a yes or no (1 or 0) diagnostic value.

A graph showing PODy for the GOES icing product based on a summation of statistics each month from July 2003 through April 2005 is shown in Fig. 6, compared with the NWS CIP (using a threshold index of 0.45) for the same period. An evaluation of the PODn for GOES versus CIP is shown in Fig. 7, while results of the TSS and ROC comparisons are provided in Figs. 8 and 9, respectively.

Improvements described in section 2 related to GOES visible data normalization and modified thresholds for *GOES-12* products implemented in late summer and fall 2003 resulted in improved PODy values

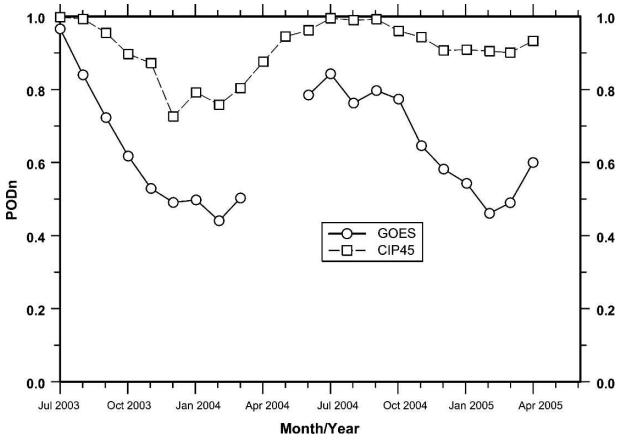

FIG. 7. Time series of the PODn for GOES (solid line) and NWS CIP (dashed) for the same period as in Fig. 8 below. Missing data for the GOES product during Apr–May 2004 were due to a local network outage. CIP results were based on a threshold index value of 0.45 as in Fig. 6.

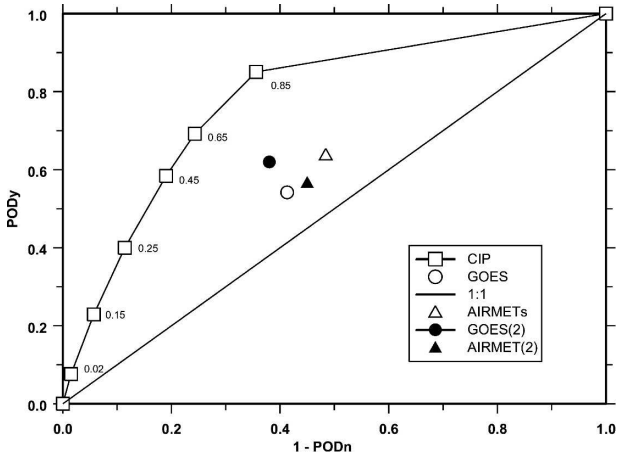

FIG. 9. ROC plots for NWS CIP, GOES icing, and NWS AIRMETs for the period from Jul 2003 through Apr 2005 (open symbols). The data points for GOES(2) (solid circle) and AIRMET(2) (solid triangle) are based on a more recent sample from May 2005 through Jan 2006 after all improvements to the GOES icing algorithm had been implemented and no further changes were made. NWS CIP results for the later period (not shown) were essentially unchanged.

(solid-line segments, open circles in Fig. 6). The GOES PODy dips during the winter months due to the increased occurrence of obscuring cloud layers, thermal inversions, etc., and increases again in spring. A correction to the band-4–6 cirrus filter was applied by February 2005 to correct an underdetection of observed icing areas. GOES PODy generally exceeds that for CIP (dashed lines), although the differences are small during the winter months. PODy for the GOES icing product was best below 3.8 km (12 000 ft) (solid circles), with values ranging from 60% to 82% through the period. These results reflect the strength of the GOES product in identifying icing conditions related to cold-air stratiform cloudiness events, that dominate during the cool seasons and are characterized by less overlying cloud cover. During summer, better GOES PODy results were due to the higher freezing level and less obscuration of supercooled clouds, despite the presence of convective icing, and corresponding cirrus cloud cover. GOES performance (PODy and TSS) during July–August of 2004 was better than in 2003 and exceeded the results for the CIP.

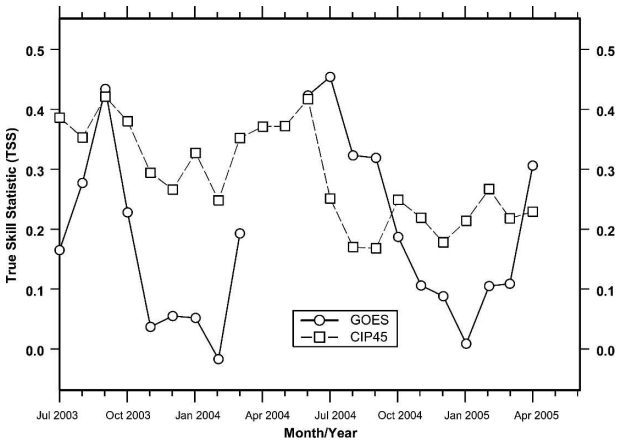

FIG. 8. TSS for GOES and CIP are shown for the same period as in Figs. 6 and 7.

Implementation of the band-4–6 cirrus filter described in section 2 (late summer 2004) was expected to reduce false alarms, and this was immediately observed qualitatively in the images as a reduction in the area of potential icing. The values of PODn (Fig. 7) for GOES were improved during the fall of 2004 when compared with a similar period in 2003. Values of PODn for the CIP (using threshold index of 0.45) were significantly better than the GOES product throughout much of the year, especially during the winter months, indicating that CIP was better able to correctly identify nonicing regions than GOES.

Statistics for TSS (Fig. 8) showed that the NWS CIP outperformed the GOES icing product significantly during the late fall and through the early spring months, although during the summer, GOES performance is equal to or better than CIP. The overall skill of both products and the Airman's Meteorological Advisories (AIRMETs) issued by NWS forecasters for the entire data period (July 2003–April 2005) is shown by the ROC plot in Fig. 9. The ROC data indicate that the experimental GOES icing potential product had skill similar to that for the AIRMETs, but significantly less than CIP during that period. ROC values for a more

recent period (May 2005–January 2006) show that the GOES product (solid circle, Fig. 11) was significantly better than for the earlier data collection period, and exhibited more skill than AIRMETs (solid triangle, Fig. 11). Results for the CIP were essentially unchanged for the later period. The likely reason for the better performance of the GOES product was that the experimental GOES algorithm with all of the improvements in place was not modified during the later period.

The underdetection of icing by the GOES product (leading to poor PODy results) is most likely due to 1) obscuration by higher cloud layers and 2) the difficulty in diagnosing icing conditions within 1–2 h of sunrise and sunset. Icing conditions will be undetected by GOES within deep frontal cloud systems whose cloud-top temperatures are $<-30°C$ (as shown in Fig. 5). PODy values during the day–night transitions (around 0000 and 1200 UTC) were typically 0.45–0.50, compared with 0.55–0.70 during daytime. Attempts to reduce this effect by compositing the icing pixels over a 2-h period and correcting the visible image data for viewing angle are not sufficient to completely eliminate this problem; thus, the product should be used with caution just before and just after sunrise and sunset.

The larger number of false alarms (larger values of 1 − PODn) compared to the CIP are related to factors such as 1) unfiltered thin cirrus that gives a positive icing test, 2) PIREPs of no icing at altitudes above a supercooled cloud (since altitude was not available for evaluation of GOES icing in RTVS), and 3) rapid passage of an aircraft through a thin supercooled cloud, thus resulting in no icing being observed, etc.

b. GOES sounder and imager cloud-top heights

The GOES CTP has been compared with data from ground-based lidar and radar systems at the Department of Energy's Atmospheric Radiation Measurement (ARM) program's Cloud and Radiation Testbed (CART) site in Lamont, Oklahoma, from April 2000 to March 2002 (Hawkinson et al. 2005). These comparisons yielded a mean height difference of 1772 m and a standard deviation of 1733 m for GOES 3 × 3 pixel fields-of-view (FOV) CTP compared with CART data (Fig. 10). The correlation between the two types of measurements was 0.836. The difference between GOES cloud-top heights and ground-based radar was ±500 m for 21% of the retrievals and ±1500 m for 60% of the retrievals. Since the current operational CTP used at NESDIS is derived from single-FOV data, the results are expected to be slightly better.

Recent intercomparisons between the GOES sounder and imager CTP's and concurrent airborne measurements from the National Aeronautics and Space Administration (NASA) Goddard Space Flight Center's cloud phase lidar (CPL) (Thomas et al. 2004) showed good correlation along the flight track, especially considering the large differences in instrument horizontal resolution (e.g., 10 km at nadir for the GOES sounder versus several meters for the CPL). However, the GOES sounder tended to underestimate CTP heights in areas of high (>10 km) and low (<4 km) clouds, with errors occasionally exceeding 5 km for high clouds. The *GOES-12* imager, using data from a new 8 km-resolution 13.3-μm CO_2 channel, was able to obtain better results than those from the sounder. For low clouds on one flight track, nearly 80% of the data points were within 1 km of the CPL, while only about 35% of the sounder points were within 1 km of the CPL. The lowest errors for both instruments were obtained for midlevel cloud layers (4 km $\leq Z \leq$ 10 km) where nearly half of the sounder observations (and over 50% of the imager heights) were within 1 km of the CPL. These results are encouraging for future use of the imager CTP in the aircraft icing product, since most icing occurs at lower altitudes.

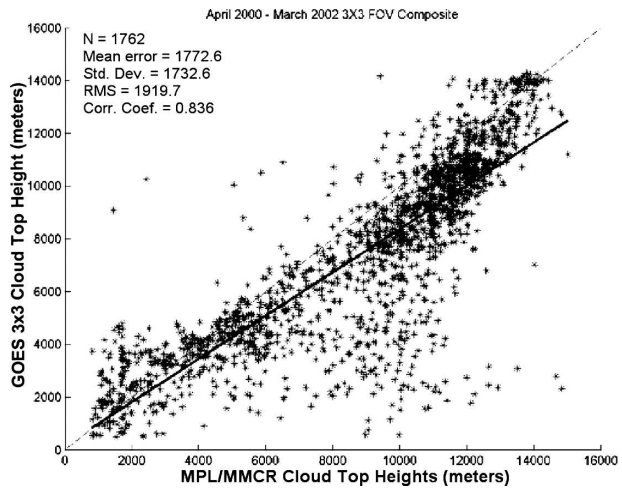

FIG. 10. Comparison of GOES cloud-top heights for a 3 × 3 pixel area vs heights determined from surface millimeter wavelength radars during the ARM CART project from Apr 2000 through Mar 2002 (from Hawkinson et al. 2005).

c. ICECAP heights versus icing PIREPs

PIREPs of moderate or greater intensity icing conditions over the CONUS were periodically collected from the GOES ICECAP images between 2 February 2005 and 11 March 2005, and then compared with GOES sounder cloud-top heights in 1.9-km (6000 ft) altitude bands. The GOES cloud-top height categories (1–4) were subtracted from the corresponding icing PIREP altitude category, and histograms were con-

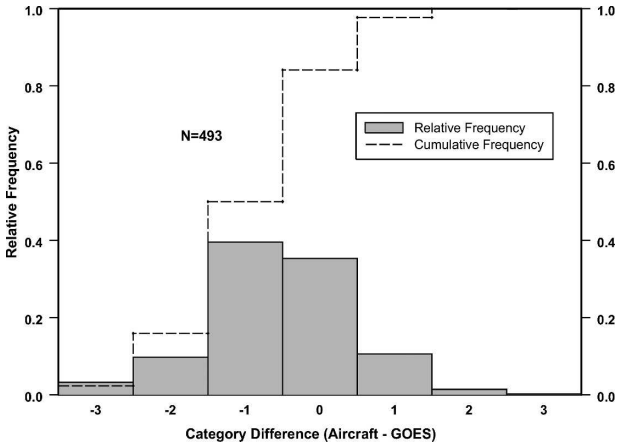

FIG. 11. Histograms showing frequency distribution and cumulative frequency of the category differences of aircraft icing altitude (from pilot reports) minus GOES cloud-top height. Each category represents a 1.9-km (6000 ft) interval between the surface and >5.7 km (18 000 ft). The "0" bar represents the number of cases where the aircraft altitude is within the same height category as GOES.

structed showing the frequencies for the resulting category differences. Since no cloud-base information is available in the satellite product, this validation simply shows whether or not the ICECAP cloud-top heights provide a reliable estimate of the approximate maximum height of potential icing conditions. Based on a total of nearly 500 observation pairs (Fig. 11), about 83% of the icing PIREP altitudes were equal to or lower than the category for the associated GOES cloud-top heights. Conversely, only about 17% of the categorized aircraft altitudes were above those from GOES, indicating that ICECAP provides useful guidance on the upper-altitude boundary of icing.

5. Proposed improvements

There are several improvements that could be considered for possible future upgrades of ICECAP. For example, the use of freezing-level heights obtained from numerical model data, possibly supplemented by satellite data in cloud-free regions, could be used in conjunction with ICECAP to estimate the depth of potential icing cloud layers. Viewing angle corrections for the 13.3-μm IR channel would improve the thin cirrus filtering from *GOES-12* (and later spacecraft possessing the same channel) for regions near the limb. Incorporation of the GOES-West imager icing product into ICECAP, in the short term at least, would likely make such a correction unnecessary, as it currently uses a split-window method (based on 11–12-μm IR BTD) that is less sensitive to viewing angle. However, there is only one more GOES spacecraft that will have the 12-μm IR band on the imager (*GOES-11*; activated on 21 June 2006) until GOES-R (~2012), so the *GOES-12* method would have to be incorporated on both -East and -West spacecraft eventually.

The use of higher-resolution polar satellite data from AVHRR or Moderate Resolution Imaging Spectroradiometer (MODIS) instruments could be exploited more fully. The latter instrument, available on the Earth Observing System *Terra* and *Aqua* spacecraft, has a full suite of 36 channels (19 visible and near-IR, 17 IR). Advanced cloud classification techniques have been developed with these data (Stowe et al. 1999) that can be utilized to identify cloud systems that may contain aircraft icing. This work would also help prepare for full exploitation of data from the Advanced Baseline imager (ABI) on GOES-R beginning around 2012 (Schmit et al. 2005).

Finally, inclusion of the altitude information contained within ICECAP into the RTVS at NOAA/FSL would likely result in improved skill scores and help to better determine the usefulness of the GOES icing product by providing additional statistics such as the percentage of airspace volume.

6. Summary and conclusions

A meteorological satellite product has been developed that displays regions of potential aircraft icing derived from the GOES imager, combined with associated cloud-top heights obtained from the GOES sounder. The combined image product, referred to as the Icing Enhanced Cloud-top Altitude Product (ICECAP), is created hourly from *GOES-12* (the operational eastern U.S. spacecraft), and is color coded to show cloud-top altitudes in 1.9-km (6000 ft) intervals. Experimental ICECAP images became routinely available on the World Wide Web during the spring of 2004. Verification of separate ICECAP components (imager icing and sounder cloud-top heights) via the RTVS indicates that the GOES product is most useful during cool seasons for icing events below 3.8 km (12 000 ft) (PODy of 55%–80%) for which there is little overlying cloud cover, but can be an effective tool during the warm season as well. GOES PODn results varied from 50% to 60% during the cool seasons to nearly 80% during the summers. There are a substantial number of "overwarned" or underdetected icing conditions by the GOES icing product, resulting in relatively poor verification results compared to the operational 40-km CIP, especially during the winter months. The overall skill of the GOES imager icing potential (as determined by

TSS and ROC) was significantly less than that for the NWS CIP for most of a 22-month period ending April 2005, but it was clear that the most recent version of the GOES algorithm has improved the skill significantly. Deficiencies of the GOES product are attributed mainly to the obscuration of supercooled clouds by higher cloud layers and the inability of the GOES technique to detect icing near sunrise and sunset because of low solar illumination. Other inherent deficiencies of the GOES product include the absence of information on icing intensity, and the inability to detect icing conditions within multilayered cloud systems. Comparison of the CTP heights with altitudes of moderate or greater icing from PIREPs indicated that the ICECAP product provides reliably accurate information on the maximum altitude of possible icing conditions. Overall, this experimental, satellite-only image product provides useful information to pilots, aviation forecasters, and dispatchers for monitoring regions of potential aircraft icing in many situations, particularly in remote areas where no other data are available.

Acknowledgments. The contents of this paper are solely the opinions of the authors and do not constitute a statement of policy, decisions, or position on behalf of NOAA or the U.S. government. The authors thank Jennifer Mahoney and the staff at NOAA/ESRL for their assistance in including the GOES imager icing product in the Real-Time Verification System and assuring continuity of the data. A McIDAS program to correct visible data for satellite viewing angle was provided by Frederick Mosher, formerly of the National Weather Service Aviation Weather Center. The software to generate the icing product was originally developed by James P. Nelson of the University of Wisconsin Cooperative Institute for Meteorological Satellite Studies (UW-CIMSS) in 1995.

REFERENCES

Allen, R. C., P. A. Durkee, and C. H. Wash, 1990: Snow/cloud discrimination with multispectral satellite measurements. *J. Appl. Meteor.,* **29,** 994–1004.

Benjamin, S., 1997: Improvements in aviation forecasts from the 40-km RUC. Preprints, *Seventh Conf. on Aviation, Range, and Aerospace Meteorology,* Phoenix, AZ, Amer. Meteor. Soc., 411–416.

Bernstein, B., F. McDonough, M. Politovich, B. Brown, T. Ratvasky, D. Miller, C. Wolff, and G. Cunning, 2005: Current icing potential (CIP): Algorithm description and comparison with aircraft observations. *J. Appl. Meteor.,* **44,** 969–986.

Curry, J. A., and G. Liu, 1992: Assessment of aircraft icing potential using satellite data. *J. Appl. Meteor.,* **31,** 605–621.

Doswell, C. A., III, R. Davies-Jones, and D. L. Keller, 1990: On summary measures of skill in rare event forecasting based on contingency tables. *Wea. Forecasting,* **5,** 576–585.

Ellrod, G. P., 1995: Advances in the detection and analysis of fog at night using GOES multispectral infrared imagery. *Wea. Forecasting,* **10,** 606–619.

——, 1996: The use of *GOES-8* multi-spectral imagery for the detection of aircraft icing regions. Preprints, *Eighth Conf. on Satellite Meteorology and Oceanography,* Atlanta, GA, Amer. Meteor. Soc., 168–171.

——, R. V. Achutuni, J. M. Daniels, E. M. Prins, and J. P. Nelson III, 1998: An assessment of *GOES-8* imager data quality. *Bull. Amer. Meteor. Soc.,* **79,** 2509–2526.

Eyre, J. R., J. L. Brownscombe, and R. J. Allam, 1984: Detection of fog at night using Advanced Very High Resolution Radiometer (AVHRR) imagery. *Meteor. Mag.,* **113,** 266–271.

Fowler, T., M. Chapman, B. Brown, and J. Mahoney, 2004: Current icing potential (CIP) severity index. Preprints, *11th Conf. on Aviation, Range, and Aerospace Meteorology,* Hyannis, MA, Amer. Meteor. Soc., CD-ROM, 9.3.

Hansman, R. J., 1989: The influence of ice accretion physics on the forecasting of aircraft icing conditions. Preprints, *Third Int. Conf. on the Aviation Weather System,* Anaheim, CA, Amer. Meteor. Soc., 154–158.

Hawkinson, J. A., W. A. Feltz, and S. A. Ackerman, 2005: A comparison of GOES sounder and cloud lidar and radar-retrieved cloud-top heights. *J. Appl. Meteor.,* **44,** 1234–1242.

Inoue, T., 1987: A cloud classification with NOAA-7 split window measurements. *J. Geophys. Res.,* **92,** 3991–4000.

Kleespies, T., 1995: The retrieval of marine stratiform cloud properties from multiple observations of varying solar illumination. *J. Appl. Meteor.,* **34,** 1512–1524.

Lee, T. F., F. J. Turk, and K. Richardson, 1997: Stratus and fog products using *GOES-8–9* 3.9 μm data. *Wea. Forecasting,* **12,** 664–677.

Mahoney, J., J. Henderson, B. Brown, J. Hart, A. Loughe, C. Fischer, and B. Sigren, 2002: The Real-Time Verification System (RTVS) and its application to aviation weather forecasts. Preprints, *10th Conf. on Aviation, Range, and Aerospace Meteorology,* Portland, OR, Amer. Meteor. Soc., 323–326.

Mason, S. J., and N. E. Graham, 1999: Conditional probabilities, relative operating characteristics, and relative operating levels. *Wea. Forecasting,* **14,** 713–725.

McDonough, F., and B. C. Bernstein, 1999: Combining satellite, radar, and surface observations with model data to create a better aircraft icing diagnosis. Preprints, *Eighth Conf. on Aviation, Range, and Aerospace Meteorology,* Dallas, TX, Amer. Meteor. Soc., 467–471.

Menzel, W. P., and J. F. W. Purdom, 1994: Introducing the GOES-I: The first of a new generation of Geostationary Operational Environmental Satellites. *Bull. Amer. Meteor. Soc.,* **75,** 757–781.

——, W. L. Smith, and T. R. Stewart, 1983: Improved cloud motion wind vector and altitude assignment using VAS. *J. Climate Appl. Meteor.,* **22,** 377–384.

——, F. Holt, T. Schmit, R. Aune, A. Schreiner, G. Wade, and D. Gray, 1998: Application of *GOES-8/9* soundings to weather forecasting and nowcasting. *Bull. Amer. Meteor. Soc.,* **79,** 2059–2077.

Petty, K. R., and C. D. J. Floyd, 2004: A statistical review of aviation airframe icing accidents in the U.S. Preprints, *11th Conf. on Aviation, Range, and Aerospace Meteor.,* Hyannis, MA, Amer. Meteor. Soc., CD-ROM, 11.2.

Politovich, M., 1996: Response of research aircraft to icing and evaluation of a severity index. *J. Aircraft,* **28,** 291–297.

Rauber, R., and A. Tokay, 1991: An explanation for the existence of supercooled water at the top of cold clouds. *J. Atmos. Sci.,* **48,** 1005–1023.

Sand, W. R., W. A. Cooper, M. K. Politovitch, and D. L. Veal, 1984: Icing conditions encountered by a research aircraft. *J. Climate Appl. Meteor.,* **23,** 1427–1440.

Saunders, R. W., and D. M. D'Aria, 1994: Emissivity of terrestrial materials in the 3–5 μm atmospheric window. *Remote Sens. Environ.,* **47,** 346–361.

Schmidt, E. O., R. F. Arduini, B. A. Wielicki, R. S. Stone, and S.-C. Tsay, 1995: Considerations for modeling thin cirrus effects via brightness temperature differences. *J. Appl. Meteor.,* **34,** 447–459.

Schmit, T. J., M. M. Gunshor, W. P. Menzel, J. J. Gurka, J. Li, and A. S. Bachmeier, 2005: Introducing the next-generation Advanced Baseline imager on GOES-R. *Bull. Amer. Meteor. Soc.,* **86,** 1079–1096.

Schreiner, A. J., and T. J. Schmit, 2001: Derived cloud products from the GOES-M imager. Preprints, *11th Conf. on Satellite Meteorology and Oceanography,* Madison, WI, Amer. Meteor. Soc., 420–423.

——, ——, and R. M. Aune, 2002: Maritime inversions and the GOES sounder cloud product. *Natl. Wea. Dig.,* **26** (1), 27–38.

Schultz, P., and M. K. Politovich, 1992: Toward the improvement of aircraft-icing forecasts for the continental United States. *Wea. Forecasting,* **7,** 491–500.

Smith, W. L., Jr., P. Minnis, and D. F. Young, 2000: An icing product derived from operational satellite data. Preprints, *Ninth Conf. on Aviation, Range and Aerospace Meteorology,* Orlando, FL, Amer. Meteor. Soc., 256–259.

Space Systems Loral, 1996: GOES I-M databook. DRL 101-08, Ref. S-415-19, 200 pp.

Stowe, L. L., P. A. Davis, and E. P. McClain, 1999: Scientific basis and initial evaluation of the CLAVR-1 global clear/cloud classification algorithm for the Advanced Very High Resolution Radiometer. *J. Atmos. Oceanic Technol.,* **16,** 656–681.

Thomas, S., W. Feltz, A. Schreiner, and R. Holz, 2004: Satellite derived CONUS cloud top pressure product validation using aircraft based cloud phase lidar data from the AtREC field campaign. Preprints, *11th Conf. on Aviation, Range, and Aerospace Meteorology,* Hyannis, MA, Amer. Meteor. Soc., CD-ROM, P8.7.

Thompson, G., R. Bullock, and T. F. Lee, 1997: Using satellite data to reduce spatial extent of diagnosed icing. *Wea. Forecasting,* **12,** 185–190.

World Meteorological Organization, 1954: Meteorological aspects of aircraft icing. WMO Tech. Note 3, WMO-30-TP9, Geneva, Switzerland, 18 pp.

Vivekanandan, J., G. Thompson, and T. F. Lee, 1996: Aircraft icing detection using satellite data and weather forecast model results. *Proc. Int. Conf. on Aircraft Icing,* Vol. II, Springfield, VA, Federal Aviation Administration, 365–373.

Wylie, D. P., W. P. Menzel, H. M. Woolf, and K. I. Strabala, 1994: Four years of global cirrus cloud statistics using HIRS. *J. Climate,* **7,** 1972–1986.